Transactions on the Built Environment vol 19, © 1996 WIT Press, www.witpress.com, ISSN 1743-3509

Microgravity test of a proof-mass actuator for active vibration control

F. Bernelli-Zazzera, M. Politano, P. Vezzosi
Dipartimento di Ingegneria Aerospaziale, Politecnico di Milano, Via Golgi 40, I-20133 Milano, Italy

Abstract

The paper presents the results of an active structural control experiment performed under microgravity conditions. The test has been conducted during an ESA parabolic flight campaign, aboard a Caravelle aeroplane. The structure is a simple cantilevered steel beam with a proof-mass actuator located at the free end. The actuator is a voice-coil linear dc motor built in house with simple and readily available components. During the microgravity phase of the parabolic flight, the structure is given an initial tip displacement, and the consequent vibration is damped by the proof mass actuator. The actuator is a highly non-linear device due mostly to the non uniform magnetic field generated by the coil and to its limited stroke, which causes early saturation of the device. So, various control laws are tested to verify if the non-linearities can be overcome. All the control laws are based on incremental position control of the mass, but in some cases an on line identification of the effective magnetic field has been performed to linearize the behaviour of the actuator. To prevent undesirable saturation, the actuator is also switched off if the mass reaches its limit positions. Interesting results are obtained, which demonstrate the effectiveness of the actuator.

1 Introduction

Researches in the field of active control of vibrations of structures in space have covered in the last three decades many important topics, among which the issue of space-borne actuators is of fundamental importance. In fact, the lack of a ground support becomes a serious concern when dealing with structural control. As reported by Hallauer [1], many different families of actuators have been developed and tested.

The easiest way to generate control forces is at the moment represented by the use of jet thrusters, which are nonetheless not suited to damp small vibrations. They are relatively simple and lightweight devices, but require fuel tanks which add weight to the structure, and they deserve refuelling in case of long mission duration.

A promising technology in great evolution is related to the so called intelligent materials, such as piezoelectric materials and shape memory alloys, deserving only electrical power which can be easily produced directly in space. Actuators based on these materials generate strains when activated and can be embedded into the structure. At the moment, the major limits of these materials are their extremely low admissible displacements (piezoelectric materials) or strains generated (shape memory alloys).

Among electrically driven actuators, proof mass (or reaction mass) actuators (PMA), have captured the interest of many research groups, and several prototypes have been built and laboratory tested by Miller [2], Zimmermann et al. [3], Haviland et al. [4], Mantegazza et al. [5] and Holloway [6]. Moreover, numerous theoretical studies performed, among the others, by Politansky and Pilkey [7], Zimmermann and Inman [8] and Lindner et al. [9], complement the knowledge of the behaviour of PMAs. In a typical PMA configuration, a mass is driven on a slide attached to the structure to be controlled, and the inertia forces generated are the actual control forces. The most efficient way to do this is to have a magnetic mass driven by a variable magnetic field. The most severe limitations of a PMA is due to the limited stroke of the mass, which does not allow control of rigid body position and limits the maximum low frequency forces applicable to very low values. Moreover, when the mass reaches its maximum stroke, undesired forces can be transmitted to the structure, with risk of destabilisation. To prevent this undesirable behaviour, suitable modifications of the control strategy must be adopted.

The mechanical design of a PMA is such that the presence or lack of gravity forces may change substantially its performances, essentially because of friction forces. So its behaviour should be verified in space rather than on ground.

In this context an existing PMA developed by Mantegazza et al. [5] has been tested under microgravity conditions, during a parabolic flight campaign organised by the European Space Agency (ESA). The structure used for the test is a simple cantilevered steel beam, with the actuator located at the free end. The size of the experiment is small enough to fit into the aircraft: the beam is 0.7 m long, with a first bending mode of the overall system just above 1 Hz, which assures a sufficient number of oscillations during the 20 seconds of microgravity available during each parabola. During the microgravity phase of the parabolic flight, the structure is given an initial tip displacement, and various control laws are tested to verify the performances of the actuator.

Transactions on the Built Environment vol 19, © 1996 WIT Press, www.witpress.com, ISSN 1743-3509

2 Mechanical design of the actuator

The actuator, developed at Politecnico di Milano by Mantegazza et al. [5], is essentially a voice coil linear DC motor. Its main components are sketched in fig. 1. The moving mass is of 0.3 kg. It is a hollow cylindrical soft iron low reluctance magnetic circuit, enclosing four high remnant permanent magnet disks in NeFeB. These interact with the current fed coil, fixed to the structure to be controlled and with a density of 19500 coils/m, generating a force along the coil axis. The mass is moveable on a linear slide, allowing a stroke of 0.025 meters. The actuator has two on-board sensors: a linear potentiometer and a servo-accelerometer, used to measure the mass position along the slide and the absolute acceleration of the controlled structure. In this configuration, colocated control laws can be implemented. The limit current fed to the coil is 2 Amperes, and the friction coefficient of the mass has been estimated to be 0.15. The nominal current-to-force gain is 4 N/A, but the actuator response is heavily asymmetric with different signs of the current, and is influenced also by the position of the mass. A second order best fit of the non-linear electromagnetic force has been determined as

$$
\begin{aligned}
F &= -0.044 - 2.7464i - 0.0193x + 0.0647ix - 0.5927i^2 + 0.0017x^2 \quad \text{for } i > 0 \\
F &= 0.2195 - 2.7907i + 0.0097x - 0.0296ix - 0.6753i^2 + 0.0029x^2 \quad \text{for } i < 0
\end{aligned}
\tag{1}
$$

where the force F is in Newton, the displacement x in millimetres and the current i in Amperes.

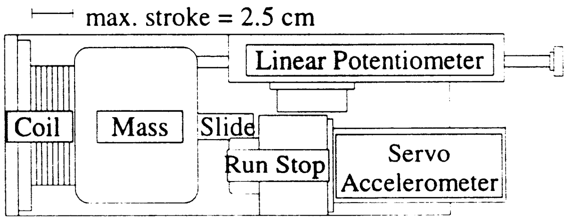

Figure 1: proof-mass actuator

3 Control law

The control law adopted is a colocated direct velocity feedback (CDVFB) (see Balas [10]), in which the velocity signal is obtained by pseudo-integration of the accelerometer signal. It is obtained in two stages. In the first stage, the displacement required to the mass to generate the commanded force is evaluated. The second stage is then a position control of the mass along the slide. Calling a_s, v_s, the acceleration and velocities of the structure, m_m, a_d, x_d the mass of the proof-mass, its desired acceleration and position, G_v and F_{com} the control gain and desired commanded force, the first stage of the controller can be written

$$v_s(s) = \left(\frac{s}{s^2 + 2\xi_f \omega_f s + \omega_f^2} \right) a_s(s) \tag{2}$$

$$F_{com} = G_v v_s \tag{3}$$

$$a_d = F_{com} / m_m \tag{4}$$

$$x_d(s) = \frac{s(s+A)}{Bs^2 + Cs + D} a_d(s) + \left(\frac{s}{s^2 + 2\xi_f \omega_f s + \omega_f^2} \right)^2 \left(a_d(s) - a_s(s)\right) \tag{5}$$

where ω_f, ξ_f are the cut-off frequency and damping of the pseudo-integrating filters, and the coefficients A, B, C, D are those of an appropriate feed-forward filter, selected in order to cancel the poles of the position control. In some conditions, the mass desired position may exceed the available stroke, so the control law must be suitably modified to prevent the mass from hitting the run stops, causing unpredictable and undesirable effects. An intuitive modification consists in saturating the desired mass position to a value slightly below the available stroke, so that in any case, even considering overshoots in the position control, it will not exceed the maximum stroke.

The second stage is implemented as a PID position control. Calling x_{pm} the actual position of the proof-mass and F_{gen} the force generated by the coil, it can be written in the form

$$F_{gen}(s) = m \frac{Bs^2 + Cs + D}{s(s+A)} \left(x_d(s) - x_{pm}(s)\right) \tag{6}$$

The force F_{str} effectively applied to the structure is then

$$F_{str}(s) = \left(\frac{s}{s^2 + 2\xi_f \omega_f s + \omega_f^2} \right)^2 F_{com}(s) + \frac{Bs^2 + Cs + D}{s^4 + As^3 + Bs^2 + Cs + D} D_e(s) + \\ + \frac{s^3(s+A)}{s^4 + As^3 + Bs^2 + Cs + D} D_i(s) \tag{7}$$

where D_e and D_i represent external and internal (e.g. friction) disturbances. Finally, the current to be fed to the coil is evaluated as

$$i = F_{gen} / G_i \tag{8}$$

where G_i may be recursively identified to take into account the non-linear behaviour of the actuator. The coefficients A, B, C, D of the polynomial determine the disturbance rejection properties of the actuator; here they have

Transactions on the Built Environment vol 19, © 1996 WIT Press, www.witpress.com, ISSN 1743-3509

been selected according to a Thomson polynomial, assuring a positioning bandwidth f_a.

$$A = 10\left(2\pi\frac{f_a}{\omega_{cut-off}}\right) \qquad C = 105\left(2\pi\frac{f_a}{\omega_{cut-off}}\right)^3$$
$$B = 45\left(2\pi\frac{f_a}{\omega_{cut-off}}\right)^2 \qquad D = 105\left(2\pi\frac{f_a}{\omega_{cut-off}}\right)^4 \tag{9}$$

In order to reduce risks of spillover, reducing at the same time the control power required by the actuator, a modification of the control law has been adopted. It consists in the application of a null control force on the beam when it is backing in to equilibrium position for the action of its elastic forces only. To do so, the mass must be kept still in an inertial frame, so its desired acceleration along the slide will be opposite to the beam tip acceleration. This prevents the mass from being shot, uselessly, to a run-stop in the direction of the movement.

A logical block scheme of the control procedure is sketched in fig. 2, while the interested reader can find a deep analysis of the control law in the paper by Mantegazza et al. [5].

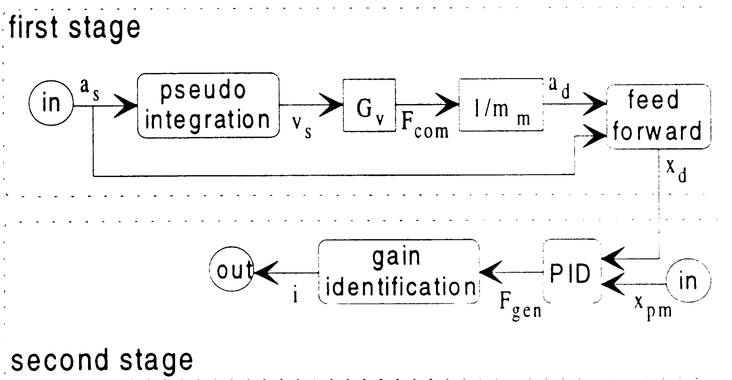

Figure 2: scheme of the control law

4 The test campaign

The flight experiments took place on a Caravelle aeroplane modified to endure the stress of parabolic manoeuvres. On board, the experiment was positioned, as shown in fig. 3, near the centre of gravity, on the left side with respect to the longitudinal axis (from fore to aft). This position is the most convenient to minimise residual accelerations, since the aeroplane is piloted according to accelerations detected by accelerometers placed on the CG. The beam was oriented along the roll axis so to have the free tip towards the plane aft. This placement was required in order to have the best microgravity level during flight and to avoid a compression load on the beam due to foreseen high accelerations along the longitudinal axis. Two investigators, placed at the sides of the equipment, were necessary in order to operate the experiment: one upstream and the other downstream, in order to have access to the free beam tip and to the computer, respectively.

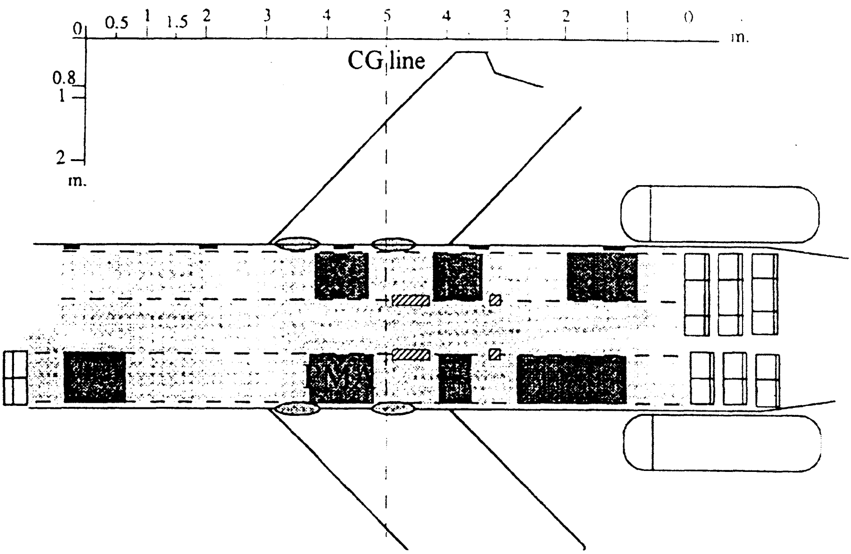

Figure 3: on board experiment position

4.1 Experiment phases

A typical parabola (see Pletser [11]) consists in a first transition, called pull-up, from level flight to a climbing hypergravity phase (1.8 g) between 7500 and 9000 meters. When the aircraft reaches a pitch angle of 50 degrees, attitude and thrust are adjusted in order to enter the parabola, and for 20 seconds the gravity level is about 0.01 g. During the parabola, the aeroplane pitch angle changes from the initial +50 to the final -50 degrees nose dive. A pull-out transition period at 1.8 g follows the parabola to return the aircraft to level flight.

The experiment phases had to follow strictly the manoeuvre events and timing. Before pull-up the beam is locked in a deflected position do to have for each test the same initial tip displacement. During the pull-up phase the data acquisition system is switched on and sensors' output stabilisation is achieved. Entering the parabola the beam tip lock is removed and a short period of free oscillations, with the mass position held by the control at the middle of the slide, is observed to check for the absence of external disturbances. After a few seconds the control is activated, and an almost complete vibration damping is achieved in about 6 seconds. Before the pull-out phase the control and data acquisition are stopped and the beam tip is re-locked in position. After returning to level flight all the data are saved on hard disk. The sequence of parabolas during the flight is very tight, with about one minute of steady flight between each parabola. This, coupled to the unusual conditions during microgravity, explain why not all the test scheduled were performed successfully.

Figures 4 and 5 show the overall experiment configuration and a picture of the actuator mounted on the beam, on board the aircraft.

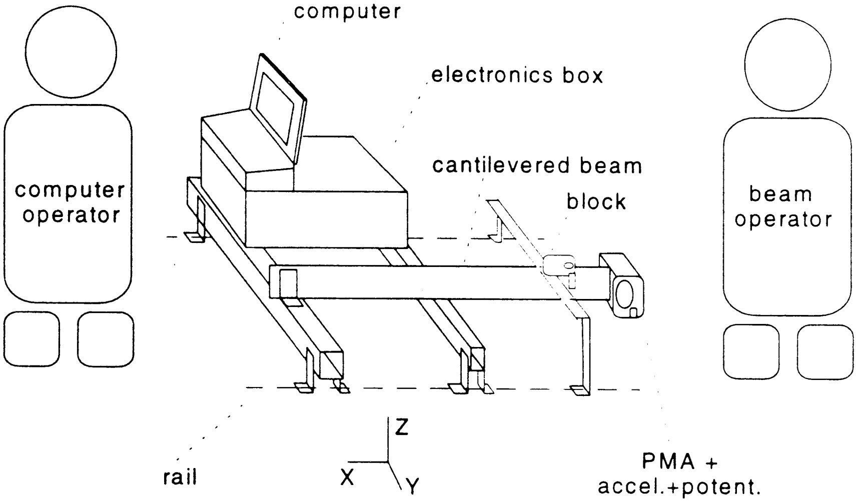

Figure 4: on board experiment configuration

Figure 5: layout of the experiment

4.2 Tests

Eight sets of eighteen tests have been executed, every time changing one of the system control parameters. Four sets were performed on ground, two on the aircraft to be used for the flight, during its ground parking time, and the last two during two different flights, in microgravity conditions.

The first six sets of experiments were used to check the overall functionality of the experiment and to gather some knowledge on the expected performances of the actuator, tuning all the control parameters.

In the eighteen tests of each set the main data have been evaluated and stored: the beam acceleration, a_s, versus time; the mass position, x_{pm}, versus time; the digital control variable evaluated, DAC, proportional with coefficient 1024 bit/ampere to the electrical current flowing in the coil; the beam tip position, x_s (obtained by a double a_s pseudo-integration); and finally, but only for the flight sets, the y and z accelerations, a_y and a_z. A typical recording is reported in fig. 6.

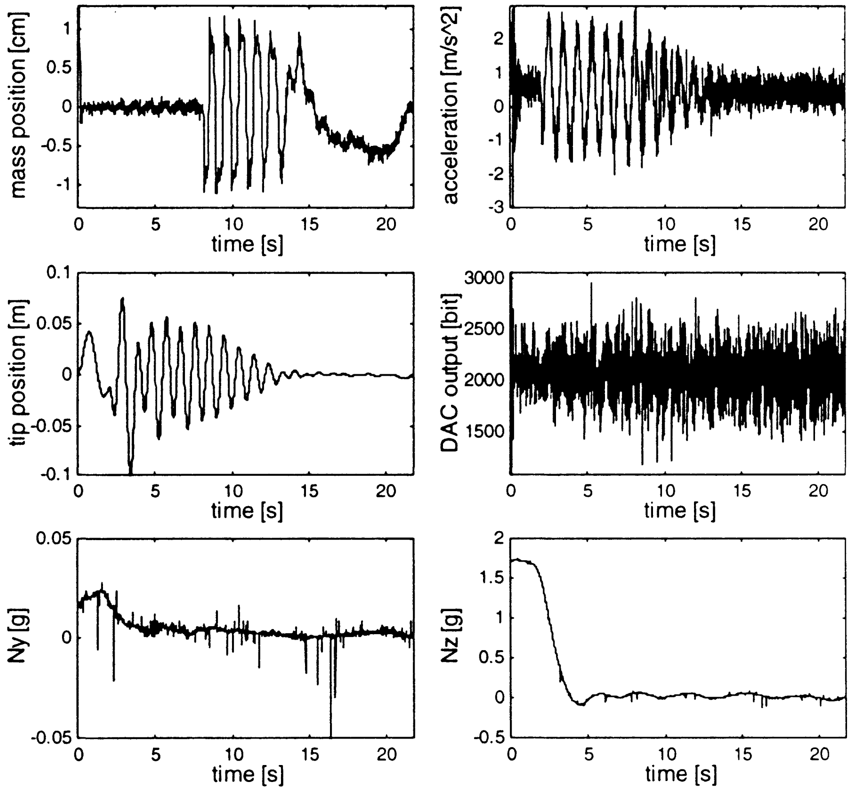

Figure 6: test data output

In the 36 experiments conducted in microgravity, four control parameters were changed to study their influence on the system performance. These parameters were chosen between the ones most affecting the system output and the optimisation requirements. In all the tests the desired mass position was saturated at ±0.9 cm, with a physical stroke saturation of ±1.25 cm, to take into account some overshoot in the position control. Performance itself was analysed evaluating three parameters which could be of fundamental importance in an optimisation index of the system. Table 1 reports a complete list of the experiments. Test number 1 was performed with the mass fixed at one end of the slide, to gather some information about the natural damping of the structure. Test number 10 instead was performed with the mass free to move along the slide, to verify the presence of friction between the mass and the coil and/or the slide. Unfortunately this test was never completed, as well as test number 12, so some conclusions will be partial.

Table 1: list of experiments performed

Test number	G_v [N/(m/s)]	Identif. method	Modified control	f_a [Hz]	Energy decay	Control cost
1		no control / mass fixed			0.031	n.a.
2	0.5	no	no	5	0.638	1.850
3	0.5	least sq.	no	5	0.625	0.852
4	0.5	max. like.	no	5	0.597	1.542
5	0.5	no	yes	5	0.738	1.507
6	0.5	least sq.	yes	5	0.800	0.755
7	0.5	max. like.	yes	5	1.070	1.435
8	0.25	max. like.	yes	5	0.932	1.506
9	1	max. like.	yes	5	0.600	1.739
10		no control / mass free			n.a	n.a
11	0.5	max. like.	yes	4	0.904	1.010
12	0.5	max. like.	yes	3	n.a.	n.a.
13	0.5	max. like.	yes	2	0.700	0.175
14	0.5	least sq.	yes	4	0.638	0.589
15	0.5	least sq.	yes	3	0.620	0.350
16	0.5	least sq.	yes	2	0.780	0.214
17	1	max. like.	yes	3	0.513	0.616
18	0.25	max. like.	yes	3	0.736	0.551

5 Analysis of results

A synthetic report of the results obtained is presented in the last two columns of tab. 1. When possible, the results represent the average of the two flight experiments with the same parameters.

5.1 Control parameters

The first control parameter investigated was the nominal frequency of the actuator position control, f_a, which influences the filtering of the system output and the amplitude of the force required on the mass. This parameter changes directly the coefficients of the feed-forward and PID stages of the control law which are calculated as values of a Thomson filter as reported in eq. (9). An increase in f_a would increase the virtual stiffness of the control and cause the requirement of greater forces on the mass. In the experiments, f_a was varied between 5 Hz and 2 Hz after many trials showing that values below 2 Hz could give forces too small to counteract external disturbances and friction and values above 5 Hz would cause the mass to be shot against the guide run-stops with great velocity. When the mass hits a run-stop it modifies the dynamics of the beam in a non-linear way and it might give energy to the system thus reducing the effectiveness of the control. The spilling of energy in modes not observed and not controlled could yield the system to instability, as discussed by Zimmermann and Inman [8].

The second control parameter analysed was the velocity gain, G_V, of the control law which influences the strength of the actuator answer. The use of a Direct Velocity Feedback control law (see Balas [10]) gives a direct influence between G_V and the damping coefficient of the dynamic equation of the controlled system thus suggesting a faster damping with higher values of the gain. In practice it has been found (see Zimmermann and Inman [8]) that high values of velocity gain could make unstable certain not controlled vibration modes. In the experiments carried out, this reduction of stability was given by the shocks the structure was subjected to when the mass hit the run-stops. In microgravity tests, G_V was varied between 0.25 N/(m/s) and 1 N/(m/s). Below those values the active damping would take too long or be ineffective and above them instability was very likely to occur.

In order to be able to increase the value of G_V without yielding instability, a modified control law was designed, as discussed in section 3. The third control parameter devised was then the switch between modified and not-modified control law.

The last choice analysed was the use of different identification methods to reduce the effect of the actuator non-linearities on the control performance. It has been shown that there are tangible differences between the control force requested to the system and the one practically obtained, because of the dependence of the output force on the mass position on the slide as well as on the value of the current commanded to the actuator, due to electromagnetic field non-linearities. These errors are not important when high values of the force are asked but are quite disturbing when a small force is required for a precise control. This event is typical after many seconds of control activation when small residual vibrations need still to be damped. In many occasions these could not be stopped for the ineffectiveness of the system control to overcome non-linearity related disturbances. The parameter identification technique allows the control law to modify the commanded current to control the mass predicting the field non-linearities and taking them into proper account. Experiments were conducted with no parameter identification, with a least squares identification method and with a maximum likelihood identification method.

5.2 Performance parameters

The first performance parameter analysed was a damping coefficient value: a fast damping is index of good performance. If the system were not affected by non-linearities, the damping coefficient would increase directly with the gain and the dynamics equation would have as a solution a sine wave damped by an exponential curve with negative exponent. Due to non-linearities, the experimental solution is a bit different from the analytical one: during the first part of control time, when the mass desired position must be often saturated, the damping of vibration is close to a Coulomb friction effect on movement (quasi-linear damping) and, after a low energy level is reached, so the mass desired position never exceeds the available stroke, the damping is fully exponential. In order to evaluate a damping parameter, an interpolation of the beam position maxima (or minima) has been carried out using an exponential curve and a least squares error fit method, see fig. 7.

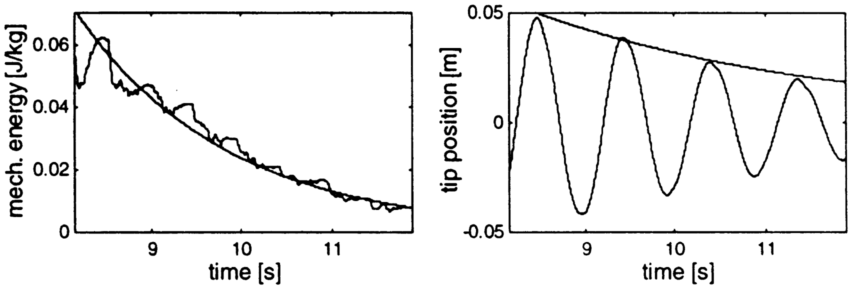

Figure 7: system damping during active control phase

Due to the small number of interpolation points (5 to 8, usually) the results were not very reliable and a more statistically significant damping parameter has been evaluated. Having the beam tip acceleration, it has been possible to calculate the velocity, the position and the frequency of vibration; with these data the value of the first mode mechanical energy in time was found. It has then been decided to use as damping performance parameter the energy decay versus time, i.e. the exponent of an exponential curve interpolating in a least squares sense the data of the first control part. Calling E_m the mechanical energy and c the damping, the following holds

$$E_m(t) = E_o e^{-ct} \tag{10}$$

$$\log(E_m(t)) = \log E_o - ct \tag{11}$$

$$y = \begin{Bmatrix} \log E_o \\ -c \end{Bmatrix} \quad ; \quad b = \begin{Bmatrix} \log E(t_1) \\ \vdots \\ \log E(t_n) \end{Bmatrix} \quad ; \quad M = \begin{bmatrix} 1 & t_1 \\ \vdots & \vdots \\ 1 & t_n \end{bmatrix} \tag{12}$$

$$y = \left(M^T M\right)^{-1} M^T b \tag{13}$$

This parameter can thus be calculated upon many hundreds of points achieving a higher statistical significance, even if it has not the meaning of damping factor of the first structural bending mode.

The second performance parameter observed was the amplitude of the residual vibration which could not be damped by the system. This vibration is due to system non-linearities and design but it can be diminished varying the control parameters. During flight, because of the short experimental time available, it was not always possible to achieve it.

The energy cost of active control was the last performance parameter analysed. It could be calculated from the values of the output command the control law gave to the actuator. These values are directly proportional to the electrical current flowing in the coil; the integral of their squares over time, normalised to the total control time, is thus related to the energy spent to control the mass.

$$\text{control cost} = \frac{1}{\left(t_f - t_o\right)^2} \int_{t_o}^{t_f} i^2 dt \qquad (14)$$

It is important to remember that no one of the performance parameters has an immediate physical meaning and that it is useful only in order to understand qualitatively how a change in a control parameter can affect performance.

5.3 General comments

The behaviour of the actuator is definitely satisfactory for a wide range of parameters. In general it can be stated that the position control of the mass can be improved further, reducing the overshoot at the imposed stroke limits (saturation of x_d) thus avoiding the slight impacts on the run stops. The non symmetric behaviour of the actuator is well evident from figs. 6, 8 and 9, where the peaks of acceleration due to physical stroke saturation occur mostly on one side. The best performances in terms of damping are obtained when the mass is driven to stroke saturation the least number of times and in the smoothest way, as evident from fig. 8. So an optimisation of the control parameters should consider this goal as primary.

5.4 Effect of the nominal frequency of the actuator on system performance

As it has been previously said, an increase in f_a yields to bigger forces and smaller displacements on the mass. This helps decreasing the residual vibration because, having smaller mass displacements the field changes due to non-linearities are less important and disturbances are more easily overcome. Unfortunately, increasing the forces required, the cost of control increases as well as can be seen from the values in tab. 1 in the analogue tests number 7,11,13 or 6,14,15,16.

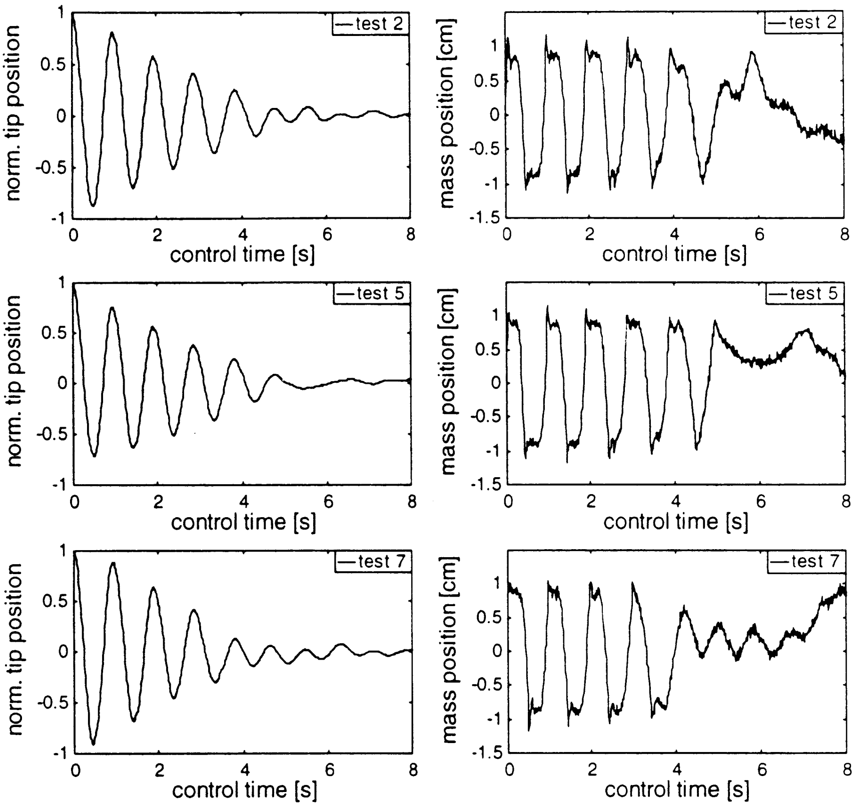

Figure 8: control performances

5.5 Effect of the velocity gain on system performance

From test 7, 8 and 9 it can be seen that a gain increase leads to a better damping until too high values are reached. Above them energy spillover or system destabilisation is likely to occur due to the mass hitting the run-stops. Higher gains yield higher forces thus overcoming the disturbances' effects and leaving smaller residual vibrations. The increase in forces requires also a higher energy cost as previously seen.

5.6 Effect of the modified law on system performance

If the modified law is adopted then it is possible to obtain higher damping because energy spillover is reduced (compare tests 2 and 5, or 3 and 6, or 4 and 7). The use of the modified law requires a lower operating cost. This because the reduction in energy spillover makes the actuator more efficient in controlling the first bending mode.

5.7 Effect of parameter identification on system performance

The parameter identification methods showed to be not useful for reducing the residual vibration. This result is neither definite nor sure because of the short observation time available for the residual vibration during microgravity. The use of least squares method lowers significantly the control cost but raises the amplitude of residual vibration: this could be related to an undershooting of the required force.

The combination of the control law modification and the parameter identification achieves the highest damping obtained. this because in such conditions the movement of the mass along the slide is somehow optimised, reducing at a minimum level the number and intensity of undesired impacts on the run stops, as evident from fig. 9. This reduces the disturbances during the early phases of the control, and stroke saturation occurs for a lower number of beam oscillations, augmenting the actuator efficiency.

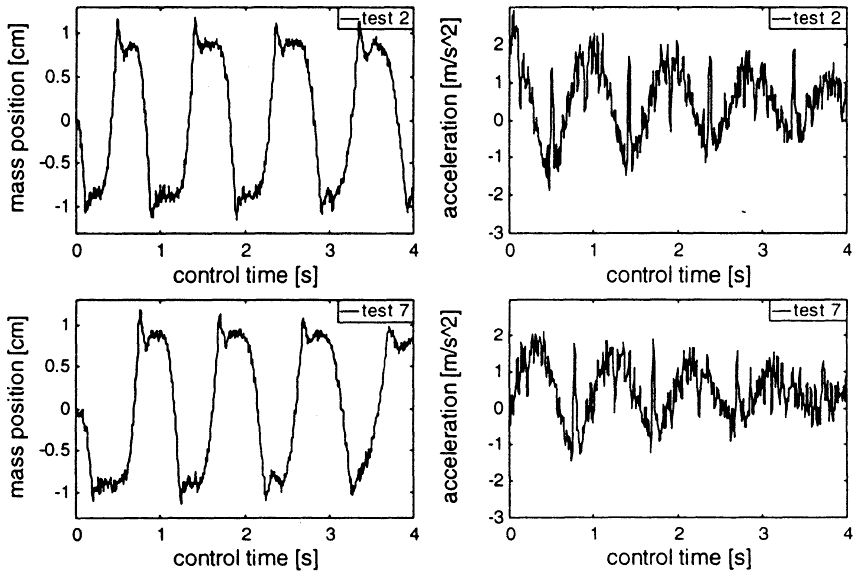

Figure 9: combined effect of gain identification and control law modification

5.8 Effect of microgravity on system performance

A sensible decrease of friction between the mass and the slide on which it runs was expected in microgravity conditions. This was supposed to affect the system performance either improving it through a better mass control or worsening it because of a lower passive energy dissipation and greater sensibility to disturbances. An attempt to compare the results of flight experiments with ground based tests has been made, but neither of the foreseen effects were found analysing the available data, and the lack of any data about test number 10 precludes a better understanding of friction effects. In any case, this negligible effect of friction forces on actuator performances can be viewed, looking at eq. (7), as an index of good disturbance rejection capabilities.

6 Conclusions

The data analysed so far strengthen the conclusion that proof mass actuators are good candidates to damp the vibrations of flexible structures. They are effective for wide ranges of their functional parameters, in spite of their intrinsic non-linear behaviour, and have good disturbance rejection capabilities. Even a simple mechanical design, aimed at minimising costs rather than maximising performances, has proven reliable. The inevitable presence of friction forces between mass and coil and/or slide, which should anyway dissipate energy in favour of vibration damping, has not been adequately characterised due to lack of data. To this end, it is suggested to have new tests carried out whose primary subject is the dynamics of the mass rather than the beam vibration control: free movement of the mass (with the actuator off) or the mass response to an impulse input should be useful in investigating the influence of friction.

Acknowledgements

The authors would like to thank Prof. Paolo Mantegazza for his useful advises, Dr. Ing. Vittorio Parma for the help provided in setting up the experiment and the European Space Agency for the organisation of the flight campaign.

References

1. Hallauer, W.L.: Recent literature on experimental structural dynamics and control research, *Mechanics and control of large flexible structures*, ed J.L. Junkins, pp. 465-489, AIAA, 1990.
2. Miller, D.W.: Dynamic profile of a prototype pivoted proof-mass actuator, *NASA CR 164861*, 1981.
3. Zimmermann, D.C., Horner, G.C. & Inman, D.J.: Microprocessor controlled force actuator, *Journal of Guidance, Control and Dynamics*, Vol.11 n.3, 1988, pp.230-236.
4. Haviland, J.K., Lim, T.M., Pilkey, W.D. & Politansky, H.: Control of linear dampers for large space structures, *Journal of Guidance, Control and Dynamics*, Vol.13 n.2, 1990, pp.234-240.
5. Mantegazza, P., Ricci, S. & Vismara, A.: Design and test of a proof-mass actuator for active vibration control, *Proceedings of the 9th VPI&SU Symposium on Dynamics and Control of Large Structures*, Blacksburg-Virginia, 1993, pp.543-557.
6. Holloway, S.E. III: Linear proof mass actuator, *NASA TM 109143*, 1994.
7. Politansky, H. & Pilkey, W.D.: Suboptimal feedback vibration control of a beam with a proof-mass actuator, *Journal of Guidance, Control and Dynamics*, Vol.12 n.5, 1989, pp.691-697.

8. Zimmermann, D.C. & Inman D.J.: On the nature of the interaction between structures and proof-mass actuators, *Journal of Guidance, Control and Dynamics*, Vol.13 n.1, 1990, pp.82-88.
9. Lindner, D.K., Zvonar, G.A. & Borojevic, D.: Performance and control of proof-mass actuators accounting for stroke saturation, *Journal of Guidance, Control and Dynamics*, Vol.17 n.5, 1994, pp.1103-1108.
10. Balas, M. J.: Direct velocity feedback control of large space structures, *Journal of Guidance and Control*, Vol.2 n.3, 1979, pp.252-253.
11. Pletser, V.: Microgravity during parabolic flights with Caravelle. ESA users' guide, *ESTEC/GP/09/VP*, Issue 2, 1989.